TÜBİTAK

Turkish Journal of Earth Sciences

Volume 33
Number 1 *SI-1*

Article 5

1-4-2024

Investigation of earthquake sequence and stress transfer in the Eastern Anatolia Fault Zone by Coulomb stress analysis

HAMDİ ALKAN
hamdialkan@yyu.edu.tr

AYDIN BÜYÜKSARAÇ
absarac@comu.edu.tr

ÖZCAN BEKTAŞ
obektas@cumhuriyet.edu.tr

TÜBİTAK

Turkish Journal of Earth Sciences

http://journals.tubitak.gov.tr/earth/

Research Article

Turkish J Earth Sci
(2024) 33: 56-68

doi:10.55730/1300-0985.1898

Investigation of earthquake sequence and stress transfer in the Eastern Anatolia Fault Zone by Coulomb stress analysis

Hamdi ALKAN[1,*], Aydın BÜYÜKSARAÇ[2], Özcan BEKTAŞ[3]

[1] Department of Geophysics, Engineering Faculty, Van Yüzüncü Yıl University, Van, Turkiye
[2] Çan Vocational School, Çanakkale Onsekiz Mart University, Çanakkale, Turkiye
[3] Department of Geophysics, Engineering Faculty, Sivas Cumhuriyet University, Sivas, Turkiye

Received: 01.03.2023 • **Accepted/Published Online:** 01.06.2023 • **Final Version:** 04.01.2024

Abstract: A devastating earthquake with a magnitude of (M_w = 7.7) occurred on February 06, 2023, in the Pazarcık segment of the Eastern Anatolian Fault Zone, which has not shown major earthquake activity for a long time. On the same day, another earthquake with a magnitude of (M_w = 7.6) occurred in Ekinözü-Elbistan (Kahramanmaraş) in the northwest. Three more earthquakes with magnitudes of M_w = 6.6, M_w = 5.9, and M_L = 5.7 occurred on the same day, and significant damage, loss of life, and property occurred in 11 provinces and districts. A sixth earthquake occurred with M_w = 6.4 magnitude in Defne-Hatay on February 20, 2023. In addition, more than 32,000 aftershocks were recorded while this study was in progress. The interconnection of these earthquakes was investigated by Coulomb stress analysis. It showed compatibility with the distribution of both these six earthquakes and small aftershocks, in which earthquakes transfer stress to each other during their formation phases. By calculating Coulomb stress changes, mainshock ruptures have played an important role in transferring stresses between Elazığ and Malatya in the northeast, Kahramanmaraş-Göksun in the west, and Hatay and Syria in the south. Also, our calculations showed that shallow depths in and around source zones received positive stress changes (~1.0 bar) due to the focal depths of mainshocks with their aftershocks. Finally, it has been better understood with these earthquakes that the stress transfer time of high-energy earthquakes can be shortened considerably.

Keywords: South Anatolia, coulomb stress analysis, earthquake, stress transfer

1. Introduction

On February 06, 2023, at 01:17:32 (UTC) in the southeast of Turkey, an earthquake with a magnitude of M_w = 7.7 occurred, which is the second-largest earthquake in Turkey in the instrumental period. The magnitude of this earthquake was measured as M_w = 7.8 by the USGS. In fact, this earthquake marked the beginning of a series of large earthquakes that occurred one after the other. Because right after, there was another aftershock with a magnitude of M_w = 6.6 at 01:28:16 (UTC). Then, on the same day approximately nine h later from the first main shock at 10:24:47 (UTC), a new mainshock of M_w = 7.6, the fourth shock of M_L = 5.7 at 10:51:28 (UTC), the fifth shock of M_W = 5.9 at 12:02:11 (UTC), and the sixth mainshock of M_w = 6.4 at 17:04:28 (UTC) occurred on February 20, 2023 (AFAD, 2023). As a result of these earthquakes, more than 50,000 people died in 11 provinces, more than 100,000 people were injured and more than 500,000 houses became uninhabitable. Considering the fault systems in which these earthquakes occurred, the fact that almost all of them are on a different fault segment raises the possibility of different mainshocks, and since this region is the East Anatolian Fault Zone (EAFZ), it can be considered as an earthquake sequence triggered by a single movement (Figure 1). The place where the first earthquake (M_w = 7.7) occurred is located within the EAFZ, as well as at the northern end of the Dead Sea Fault Zone (DSFZ) (Figure 2). As a result of the complex tectonic structure of the region, earthquakes have occurred in relation to each other. Due to its left-lateral strike-slip and the approximately 580 km long EAFZ character, it transmits stress to the next segment after each earthquake that occurs in its segments. The tectonic system that Turkey is in has led to the formation of the EAFZ and the North Anatolian Fault Zone (NAFZ), and they have been the main reason for the westward movement of the Anatolian Plate geodynamically (Şengör et al. 1985; McClusky et al. 2000; Bozkurt 2001; Reilinger and McClusky, 2011).

Many researchers have conducted studies at different levels, mostly drawing attention to earthquake hazards

* Correspondence: hamdialkan@yyu.edu.tr

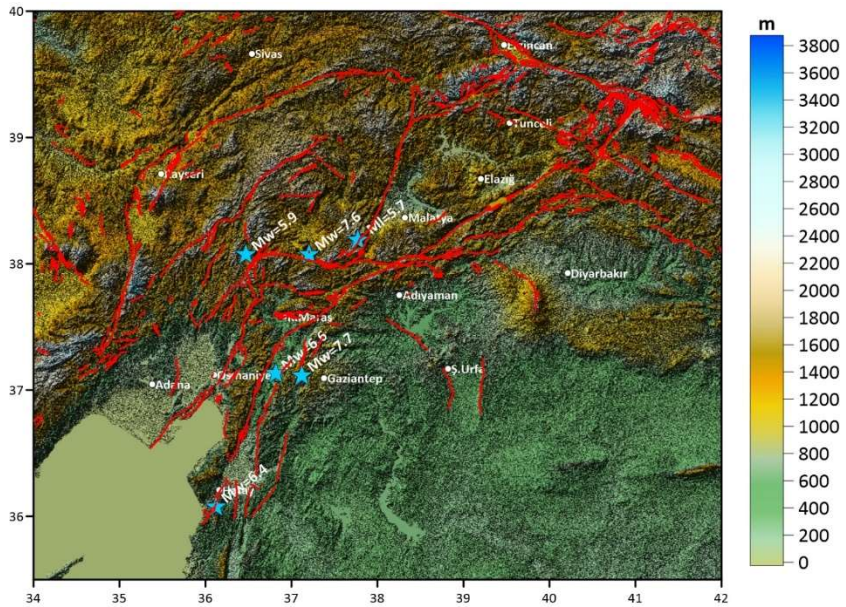

Figure 1. Epicentral distributions of earthquakes dated the 06th of February 2023 and 23rd of February 2023.

in the EAFZ. For example, Bayrak et al. (2015) calculated the *b*-value along the EAFZ and determined that the lowest *b*-value was around Karlıova. Irmak et al. (2021) concluded that the westward movement of the Central Anatolian High Plateau of January 24, 2020, Sivrice (Elazığ) earthquake (M_w = 6.8) included not only the left lateral strike-slip movement of the EAF but also the extensional transtensional movements of the upper crust within and along the EAFZ. The expectation of an important earthquake in the EAFZ has been revealed in many studies. Lower *b*-values were observed in the NE section of the EAFZ compared to the SW section. Although the relatively high *b*-value in the Gölbaşı-Türkoğlu segment, which is considered to be a seismic gap in particular, creates a contradiction, the reason for this is that there were many low-magnitude earthquakes in the region between the dates studied (Kartal and Kadirioğlu, 2013). Gülerce et al. (2017) created the probabilistic seismic-hazard assessment maps for EAFZ. They calculated *b*-values around the rupture systems along the EAFZ. The low *b*-values (~0.81) were generally obtained for the whole of EAFZ, the smaller of which (~0.6) was calculated for the Ilıca-Karlıova region which has higher stress levels. Considering the stress transfer and future hazard forecast, Öztürk (2020) inferred that the seismic *b*-values showed a decreasing trend (~0.55) calculated in and around the Central Anatolian region, especially Kahramanmaraş. On the other hand, significant seismic quiescence areas included the west of Malatya and Kahramanmaraş. Coulomb analysis conducted by Alkan et al. (2021) after the January 24, 2020, Sivrice (Elazığ) earthquake (M_w = 6.8) related to stress transfer and segments triggering each other in the EAFZ, stated that the next earthquakes are expected between Adıyaman, Diyarbakır and Elazığ, Bingöl in the northeast of Kahramanmaraş. In the study carried out by examining the focal depths of earthquakes occurring in the EAFZ, it was observed that small and medium-sized earthquakes migrated from the main fault to adjacent fault segments systematically (Bulut et al., 2012). Duman and Emre (2013) determined that the Pötürge, Pazarcık, and Amanos fault segments along the EAFZ have the potential to produce large earthquakes in the near future. In this study, the Coulomb stress analysis method was used to determine the expected earthquake hazard locations in the EAFZ. The results of the method are sensitive to the history of major earthquakes in the region, and detailed studies are needed to define the exact rupture geometries of previous earthquakes in these segments (Nalbant et al., 2002).

2. Seismotectonics of the East Anatolian Fault Zone

When the tectonic system in Turkey is examined, the Arabian Plate, which is a part of the African Plate, moves north to the Eurasian Plate, compressing Eastern Anatolia, and with the effect of this compression, the NAFZ and the EAFZ effect, it is seen that the Anatolian Plate moves westward (Figure 2). The EAFZ, with an average length of 580 km, is one of the most seismically active regions of Turkey and many major earthquakes have occurred along this fault zone. The EAFZ is a left-lateral strike-slip fault, forming

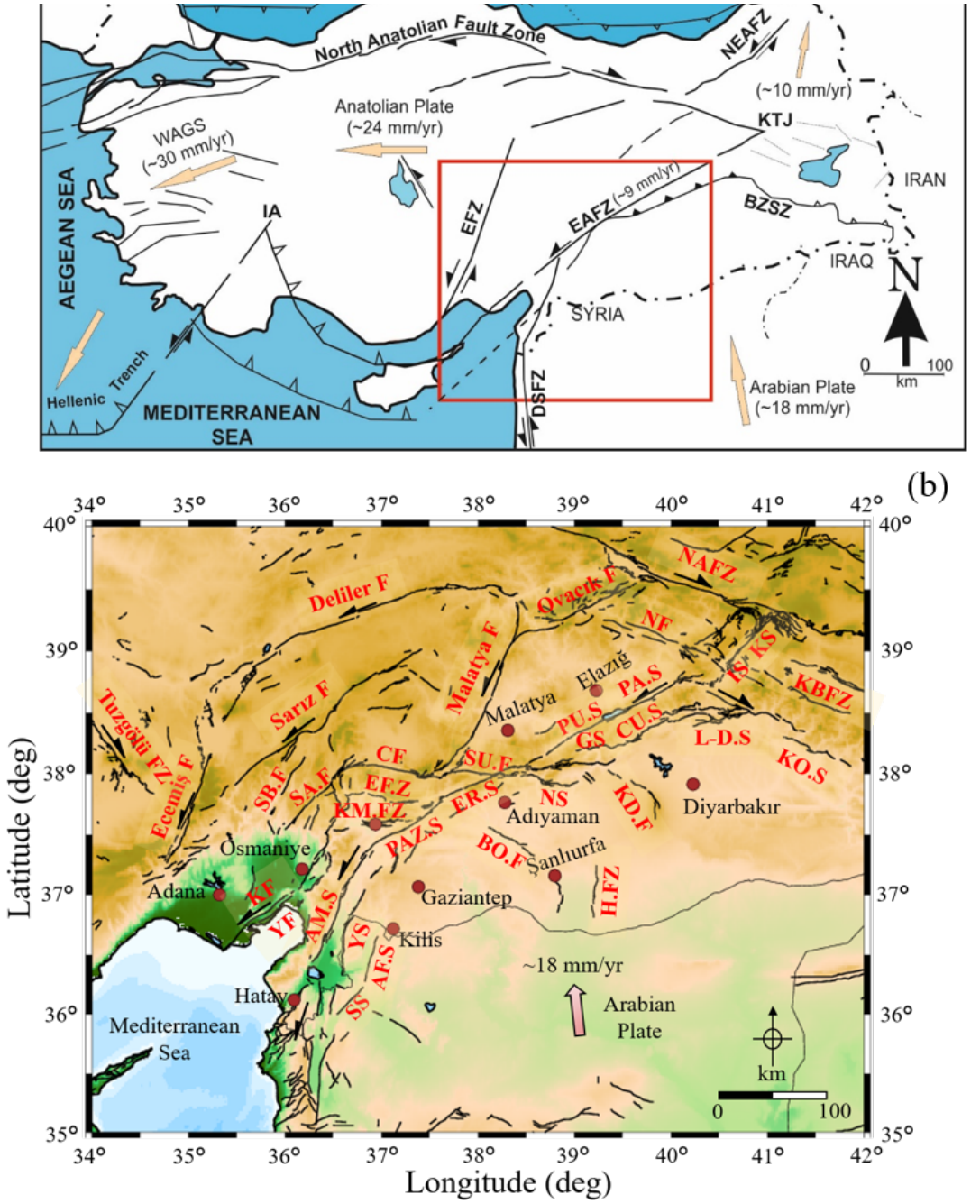

Figure 2. (a) Active tectonic map of Arabian and Anatolian Plates (modified from Okay and Tüysüz (1999), Alkan et al. (2021)). Yellow arrows indicate plate velocities (mm/yr). The red rectangle shows the study region. Abbreviations; *EBSB*: East Black Sea Basin, *MBSR*: Middle Black Sea Ridge, *WBSB*: West Black Sea Basin, *NEAFZ*: Northeast Anatolian Fault Zone, *WAGS*: West Anatolian Graben System, *KTJ*: Karlıova Triple Junction, *EAFZ*: East Anatolian Fault Zone, *BZSZ*: Bitlis-Zagros Suture Zone, *DSFZ*: Dead Sea Fault Zone, *EFZ*: Ecemiş Fault Zone. (b) The main tectonic elements and active fault segments along with the East Anatolian Fault Zone (modified from Reilinger et al. (2006) and Emre et al. (2018)). The black lines delineate the major active faults. The dark red circles denote city centers. Abbreviations; *AF.S*: Afrin Segment, *AM.S*: Amanos Segment, *BO.F*: Bozova Fault, *CF*: Çardak Fault, *CU.S*: Çürgüş Segment, *IS*: Ilıca Segment, *L-D.S*: Lice-Dicle Segment, *E.FZ*: Engizek Fault Zone, *ER.S*: Erkenek Segment, *GS*: Gerger Segment, *H.FZ*: Harran Fault Zone, *KBFZ*: Kavakbaşı Fault Zone, *KM.FZ*: Kahramanmaraş Fault Zone, *KD.F*: Karacadağ Fault, *KF*: Karataş Fault, *KO.S*: Kozluk Segment, *KS*: Karlıova Segment, *NF*: Nazimiye Fault, *NS*: Narince Segment, *NAFZ*: North Anatolian Fault Zone, *PA.S*: Palu Segment, *PAZ.S*: Pazarcık Fault, *PU.S*: Pütürge Segment, *SA.F*: Savur Fault, SB.F: Saimbeyli Fault, *SS*: Sermada Segment, *SU.F*: Sürgü Fault, *YF*: Yumurtalık Fault, *YS*: Yesemek Segment.

the southeast boundary of the Anatolian plate and intersecting the NAFZ at Karlıova. Similarly, the EAFZ merges with the DSFZ around Antakya (Figure 2). On the other hand, it basically extends from Karlıova to İskenderun Bay in the southwest direction with seven different segments (Figure 3) (Emre et al., 2018; Alkan et al., 2021). Large and destructive earthquakes occur along these faults, which are of strike-slip character (Ergin et al., 1967; Over et al., 2002). Both historical and instrumental records reveal that this region has been affected by devastating earthquakes for nearly 2000 years (Willis, 1928; Sieberg, 1932; Ergin et al., 1967; Ambraseys, 1970; Poirier and Taher, 1980; Soysal et al., 1981; Ambraseys and Barazangi, 1989). Important earthquakes that occurred in the historical period on the segments forming the EAFZ were respectively 29 November 1114 (M > 7.8), 28 March 1513 (M > 7.4), 1822 Antakya Earthquake (M_S = 7.5 approximately 200 km surface rupture), 1866 Karlıova-Bingöl Earthquake (M_S = 7.2 approximately 45 km surface rupture), 1872 Amik Lake earthquake (M_S = 7.2 approximately 20 km surface rupture), 1874 and 1875 Hazar Lake earthquakes (M_S = 7.1 and M_S = 6.7, 45 and 20 km surface rupture) and 2 March 1893 Malatya Earthquake (M_S = 7.1) (Ambraseys and Jackson, 1998) (please see details in supplementary material; Table S1). In the instrumental period 04.12.1905 (M_S = 6.8), 28.09.1908 (M_S = 6.1), 20.08.1966 (M_S = 6.2), 22.05.1971 (M_S = 6.8), 27.01.2003 (M_d = 6.1), 08.03.2010 (M_L = 5.8), and 24.01.2020 (M_W = 6.8) earthquakes did occur, but these earthquakes were not as destructive as historical earthquakes (please see details in supplementary material; Table S2). Çetin et al. (2003) interpreted the seismic quiescence along the entire EAFZ as that the fault was locked for this period. Historical earthquakes start from the NE end of the EAFZ and continue toward the SW. The general distribution of historical earthquakes is concentrated in the middle and SW parts of the EAFZ (Figure 3).

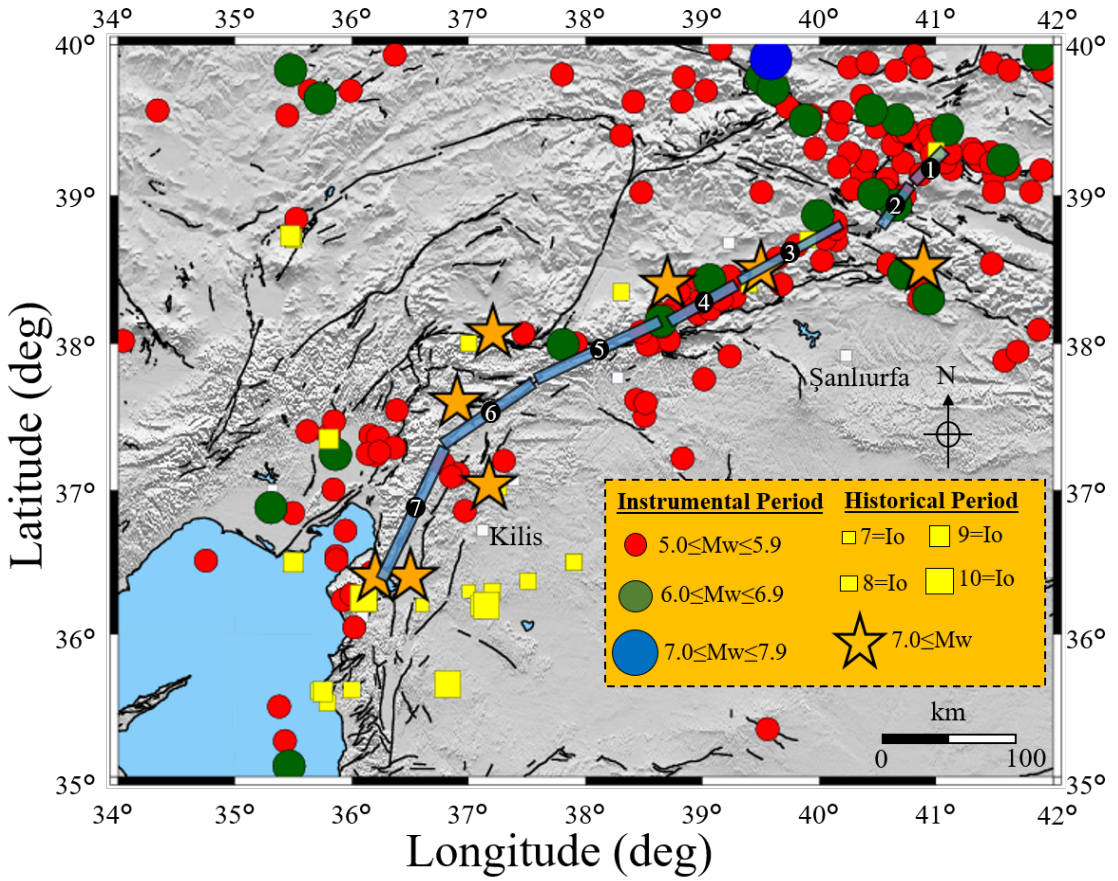

Figure 3. Historical (between 69–1895 AD) and instrumental (between 01 January 1900 –05 February 2023) earthquakes in and around the Eastern Anatolian Fault Zone (compiled from AFAD website (https://deprem.afad.gov.tr/event-historical and https://deprem.afad.gov.tr/event-instrumental). Orange stars symbolize destructive earthquakes. The map also depicts the fault segments of the East Anatolian Fault Zone (*1: Karlıova segment, 2: Ilıca segment, 3: Palu segment, 4: Pütürge segment, 5: Erkenek segment, 6: Pazarcık segment, 7: Amanos segment*).

On the Gölbaşı-Türkoğlu segment, where the fault folds into the SW, there has not been a devastating earthquake for the last 500 years to cause a surface rupture.

GPS studies show a slip rate of 9–10 mm/year for the EAFZ (McClusky et al., 2000; Reilinger et al., 2006; Aktug et al., 2016). About one-third of this is shared by the northern coast after bifurcation (Westaway, 2004; Altunel et al., 2009; Mahmoud et al., 2013; Emre et al., 2013).

The last devastating earthquake in this region occurred in 1872 and its acceleration was estimated to be 0.4 g (Över et al., 2004). After the previous earthquakes along the EAFZ and the M_W = 6.8 earthquake in Sivrice (Elazığ) in 2020, it was stated that an earthquake was expected by pointing out a seismic gap in this area, on which many researchers agree (Nalbant et al., 2002; Duman and Emre, 2013; Alkan et al., 2021).

3. Stress transfer

In fact, the phenomenon called stress transfer, which is considered under the name of triggering after an earthquake occurs at a point, is defined as the transfer of the energy of a moving part to another part in conditions where there is more than one fault system in a fault zone. The most common representation of elastic stress interaction is based on the calculation of Coulomb stress changes caused by earthquake dislocations (Harris, 1998; King and Cocco, 2001). Coulomb stress variations are widely used in the literature to investigate fault interactions between major earthquakes and also to model aftershock models and seismicity rate changes over longer time windows. Despite the large number of observations that trigger earthquakes, many questions remain unanswered about the physical mechanisms that could explain earthquake formation and the spatio-temporal pattern of seismicity. In particular, it is well known that other time-dependent processes such as aftershock, viscoelastic relaxation of the lower crust, and fluid flow can alter the induced coseismic stress field. These stress perturbations occur at different temporal scales. By limiting the analysis to the aftershock duration, pore fluid flow can play a dominant role in inducing seismicity. Propagation processes of pore pressure relaxation in fractured and saturated rocks have been proposed to explain both earthquakes and triggered seismicity (Shapiro et al., 2003; Antonioli et al., 2005).

The focal mechanism solution of the earthquakes, the details of which are given in Table, showed that the earthquakes in Pazarcık and Elbistan segments belong to strike-slip, the segment where Yeşilyurt earthquake is located to dip-slip reverse faulting, Göksun earthquake to normal faulting, and Defne earthquake to strike-slip faulting (Figure 4). More than 9000 aftershocks have occurred from these earthquakes.

4. Coulomb stress analysis

Investigation of areas that are likely to experience earthquakes in the future is one of the important stages of earthquake hazard determination. To reach this goal, the processes that create the earthquake should be well known. Stress changes in active faults due to earthquakes are decisive for the estimation of dangerous zones. An earthquake can lead to the normal occurrence of earthquakes that may occur after it, delay it, or trigger other faults (Stein et al., 1997; Çakır et al., 2003; Nalbant, 2005). Stress accumulation occurs in fault zones depending on tectonic processes, and these stresses decrease with the occurrence of earthquakes. When there is an earthquake, the earthquakes that occur with the movement in the relevant fault reduce the tension in the region. After the stress reduction, the earthquake hazard decreases until a new stress accumulation occurs (Chinery, 1963). The increase in the tension in the region due to the earthquake action causes the nearby faults to be triggered. The decrease or accumulation of ten-

Table. Source parameters of six induced earthquakes. The fault plane solutions are compiled from the AFAD website (https://deprem.afad.gov.tr/event-catalog).

No	Date (UTC)	Latitude (°N)	Longitude (°E)	Depth (km)	Magnitude Type		Location	S/D/R (°)	Source
1	06-02-2023 01:17:32	37.288	37.043	8.6	M_W	7.7	Pazarcık (K.Maraş)	233/74/18	AFAD
2	06-02-2023 01:28:16	37.304	36.920	6.2	M_W	6.6	Nurdağı (Gaziantep)	187/43/-30	AFAD
3	06-02-2023 10:24:47	38.089	37.239	7.0	M_W	7.6	Elbistan (K.Maraş)	90/86/13	AFAD
4	06-02-2023 10:51:28	38.311	38.191	7.0	M_L	5.7	Yeşilyurt (Malatya)	241/33/107	AFAD
5	06-02-2023 12:02:11	38.071	36.478	17.04	M_W	5.9	Göksun (K.Maraş)	9/56/-95	AFAD
6	20-02-2023 17:04:28	36.121	36.074	16.74	M_W	6.4	Defne (Hatay)	214/57/-44	AFAD

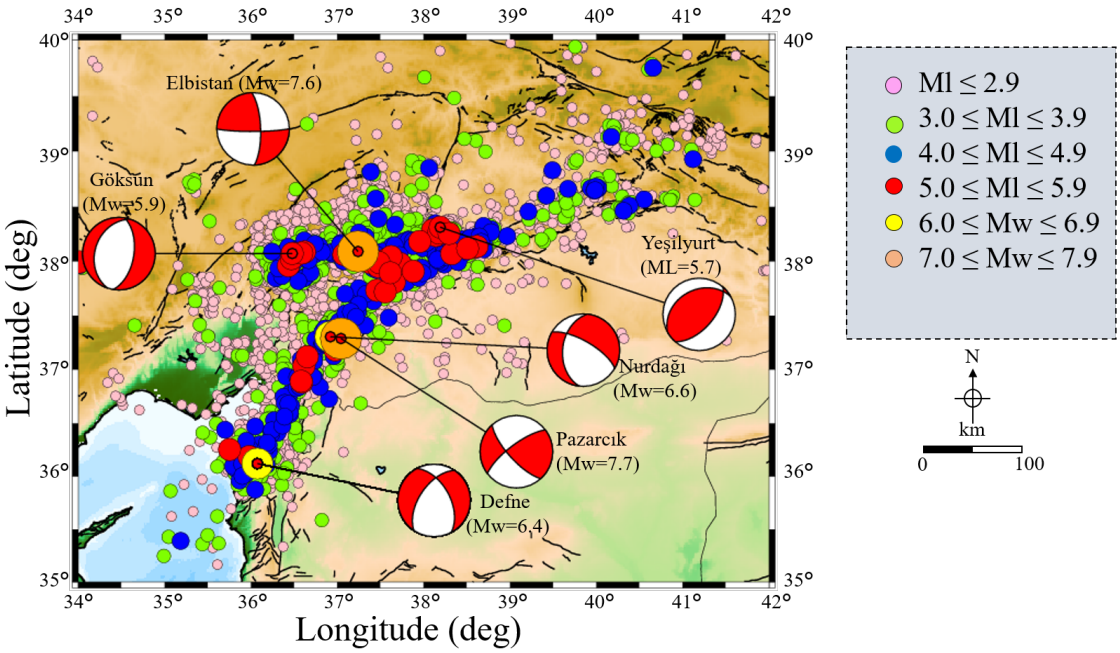

Figure 4. Epicenter distribution of the Pazarcık earthquake (M_W = 7.7), Nurdağı earthquake (M_W = 6.6), Elbistan earthquake (M_W = 7.6), Yeşilyurt earthquake (M_L = 5.7), Göksun earthquake (M_w = 5.9), and Defne earthquake (M_w = 6.4), and their aftershocks from February 06, 2023 to February 27, 2023. The magnitudes of the earthquakes are depicted with different circular symbols. The fault plane solutions of mainshocks are taken from the AFAD website (https://deprem.afad.gov.tr/event-catalog). The earthquake database is compiled from Kandilli Observatory and Earthquake Research Institute (http://www.koeri.boun.edu.tr/sismo/2/en/).

sion in the region is possible by observing the Coulomb stress variation.

Earthquake and fault relationship can be established and the earthquake hazard in the region can be calculated by determining the Coulomb stress variation (Toda et al., 1998). Displacement in an active fault with the potential to produce earthquakes causes static stress changes. The displacement in this elastic half-space is used to calculate the 3D stress field and multiplied by the elastic stiffness to derive the stress changes. The Coulomb stress variation depends on the geometry and slippage of the earthquake, the geometry of the fault and the sense of slip, and the effective friction coefficient (Stein et al., 1994). The Coulomb failure stress change (**ΔσCFS**) caused by a source earthquake on an adjacent receiver fault can be expressed as

$$\Delta\sigma_{CFS} = \Delta\tau + \mu'\Delta\sigma_n \quad (1)$$

where $\Delta\sigma_{CFS}$ is the critical Coulomb failure stress on a receiving fault, is the shear stress change on a given fault plane (assumed positive in the direction of fault slip), is the normal stress change (positive when unclamped) and μ' is the effective friction coefficient. The effective friction coefficient is dimensionless and varies between 0.2 and 0.8 for the continental structures. The effective friction coefficient in this study was assumed as $\mu' = 0.4$ due to the continental strike-slip fault mechanisms. In addition, Young's modulus was used as $E = 80\ GPA$ with Poisson's ratio of $m = 0.25$ for the elastic half-space (King et al., 1994; Lin and Stein, 2004; Toda et al., 2011). When a fault slip occurs during an earthquake, the surrounding environment is deformed, and the stress field changes (Ansari, 2016). Stress triggering describes the sensitive rupture of faults resulting from increases in Coulomb stress caused by extrinsic deformation events (King et al., 1994). Although adjacent displacements generally yield small-scale stress changes, the fields of deteriorated Coulomb stress states have been successfully used to explain the distribution of stress-induced aftershocks. On June 28, 1992, approximately three h after an earthquake (M = 7.3) near Landers, California, 40 km away, the Big Bear aftershock (M = 6.5) occurred. The calculated Coulomb stress changes from both of these earthquakes showed a western lobe increasing Coulomb stress of 2.1–2.9 bar, which was due to the displacement associated with both earthquakes. More than 75% of the approximately 20,000 aftershocks within a 5 km radius after 25 days occurred in areas of increased Coulomb tension and the remainder in areas of decreased Coulomb tension. Another example, though extended over a longer period of time, was 13 earthquakes ($M \geq 6.6$)

along the North Anatolian Fault System from 1939 to 1999, which occurred along Turkey's NAFZ.

Eleven of these earthquakes occurred in areas of increased Coulomb tension caused by a previous rupture (Stein et al., 1997; Barka et al., 1999). Similarly, it is a known fact that earthquakes occurring along the East Anatolian Fault Zone are segments that trigger each other and create stress.

5. Results and discussions

The transfer of the energy of a moving segment to another segment after an earthquake occurs in one segment in a multi-segment fault system has become a common phenomenon observed in many parts of the world. NAFZ and EAFZ are two well-known examples of these situations in Turkey. The direction and orientation of elastic stress interaction can be determined by calculating Coulomb stress changes. The results of the Coulomb stress analysis performed after the 24 January 2020 Sivrice-Elazığ earthquake (M_w = 6.8) clearly showed that the stress was transferred to the next segments, Adıyaman and Kahramanmaraş in the southwest (Alkan et al., 2021). The occurrence of very destructive earthquakes in these segments after about three years is understood as an expected situation in this sense. Stress modeling of six earthquakes, which started with the earthquake (M_w = 7.7) in Pazarcık-Kahramanmaraş on 06 February 2023 and triggered each other for very short periods, was carried out with Coulomb 3.3 software (Toda et al., 2011). The important parameters to calculate the Coulomb stress change of an earthquake are the location (latitude and longitude in degree), depth (km), magnitude, dip (degree), strike (degree), and rake (degree). These parameters are very vital to eliminate uncertainties regarding the parameters of the Coulomb stress analysis. For three-component seismograms (Z, N, and E) of a large earthquake, it is generally a less complex problem to mark the P- and S-phases, determine the maximum amplitudes of the P- and S-phases, and specify the coda length of the seismograms. Therefore, the focal mechanism solutions calculated by the AFAD or other seismology institutes such as the USGS or the KOERI can be reliable. In this study, hence, we created the Coulomb stress change maps and cross-sections using the focal mechanism solutions of AFAD.

The results show that the earthquakes after the first main shock occurred in the areas where Coulomb stress increased. Coulomb stress analysis performed at four different depths (5, 10, 15, and 20 km) for the first main shock (M_w = 7.7) and the aftershock (M_w = 6.6) that occurred afterward, indicates that the stress was increased Malatya-Adıyaman in the northeast, Elbistan-Göksun in the northwest, Hatay-Syria border in the south and İskenderun Bay in the southwest directions (Figure 5). Especially in the shallow depths of the crust (~10 km), it can be observed that the stress values are quite high (~0.1 bar) both along the fault zone and along the four different directions mentioned. On the contrary, the stress values along the city centers of Adana and Osmaniye, east of Gaziantep and north of Kahramanmaraş are low (~-0.1 bar) between 0–20 km depth. On the other hand, positive stresses along the Yumurtalık fault and the Karataş fault were observed to be transferred towards the Cyprus trench in the southwest. After the first two earthquakes (M_w = 7.7 and M_w = 6.6), the main shock (M_w = 7.6) that occurred and was triggered in Ekinözü-Elbistan (Kahramanmaraş) and the other earthquakes Yeşilyurt (Malatya) (M_L = 5.7), Göksun (Kahramanmaraş) (M_w = 5.9) (Figure 6) and Defne-Samandağ (Hatay) (M_w = 6.4) earthquakes occurred in regions where stress is positive (Figure 7). Coulomb stress analysis of the Ekinözü-Elbistan (M_w = 7.6), Yeşilyurt-Malatya (M_L = 5.7), and Göksun-Kahramanmaraş (M_w = 5.9) earthquakes, which are the next three earthquakes occurring in different segments following the M_w = 7.7 main shock and the M_w = 6.6 aftershock, was performed and it was clearly seen that it was transferred to the **Çüngüş**, Palu, and Pazarcık Segments located between Elazığ and Diyarbakır in the east and to the Sarız Fault and Ecemiş Fault in the west. The aftershock sequences that occur after the main shocks also confirm this energy transfer. On the other hand, as an important note, a stress increase was observed towards Malatya and Ovacık faults at 0–20 km depth in the north and between Gaziantep and Kilis in the south (Figure 6).

The current stress situation has become clear as a result of the combined Coulomb analysis of six earthquakes, which were included in the Defne-Hatay earthquake (M_w = 6.4) that occurred on the 20th of February, 2023. According to this, the stresses (~0.1 bar) were positively transferred regions observed at a depth of 0–20 km around the İskenderun Bay in the southwest, towards Karlıova triple junction along Elazığ-Malatya in the northeast, along the Kahramanmaraş fault zone between Kahramanmaraş-Göksun in the west, along the Hatay-Syria border in the south, that is, in the region where the segments of the EAFZ and DSFZ intertwine. Considering the epicenters of more than 9000 aftershocks, it can be assumed that stress transfers will continue in these directions (Figure 7).

In addition, the vertical displacements of the focal mechanism solution of M_w = 7.7 and M_w = 7.6 magnitudes of the two mainshock solutions using Coulomb 3.3 software (Toda et al., 2011) are given in Figure 8 and Figure 9, respectively, and the horizontal displacement diagrams are given in Figure 10a and 10b, respectively. When Figure 8 and Figure 9 are examined, vertical cross-sections were obtained for the 0–30 km depth range along the A-B profiles. In the sections formed along the fault zones, the yellow circles represent the epicenter point in both earthquakes.

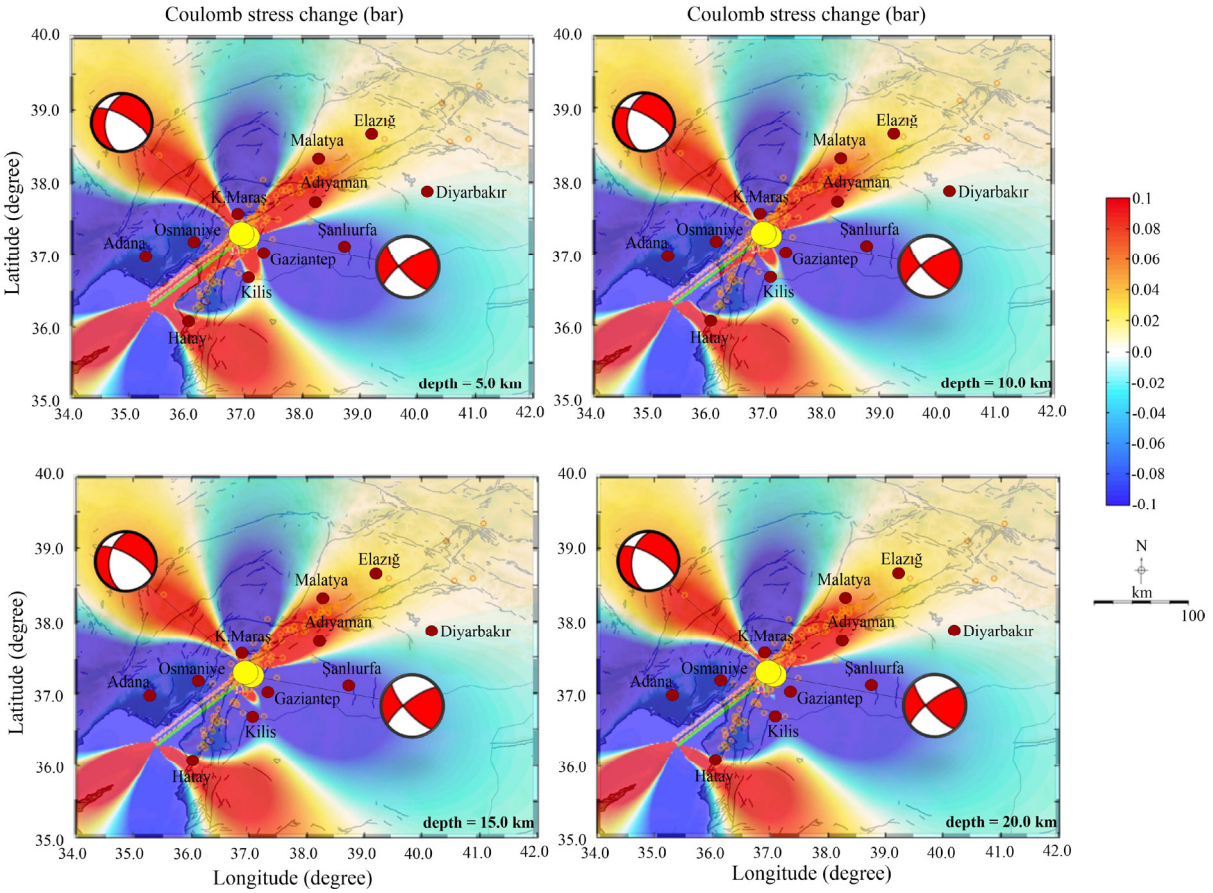

Figure 5. Coulomb stress changes due to the first main shock and aftershock (M_w = 7.7 and M_w = 6.6) occurred around the Pazarcık for the depths of 5.0, 10.0, 15.0, and 20.0 km. The big yellow circles show the epicenter of the main shocks with the focal mechanism results taken from the AFAD website (https://deprem.afad.gov.tr/event-catalog). The orange circles depict epicentral locations of aftershocks that occurred from 06.02.2023 at 01:17:32 (UTC) to 06.02.2023 at 10:24:47 (UTC). Claret red circles show the city centers. Black lines represent the active faults (modified from Emre et al. (2018)).

The first main shock coincides with the Narlı Segment at the northern end of the DSFZ, while the second main shock coincides with the Çardak Fault of the EAFZ. Considering the general stress characteristics in both sections, low stress around the hypocentral region and high-stress transfer along the fault zone in the NE-SW direction for the first main shock and in the E-W direction for the second main shock emerged. The stress characteristic of these two main shocks generally reflects the entire energy system of the region. On the other hand, horizontal displacement vectors obtained from focal mechanism solutions of the Disaster and Emergency Management Authority (AFAD) (Table) for both main shocks are shown in Figures 10a and 10b. Besides, in the horizontal displacement calculation, the medium, which controls the environmental propagation of the earthquake source's impact, is assumed uniform (Yildiz et al., 2021). According to the solutions obtained, the character of both earthquakes supports the solution of the left-sided focal mechanism. In addition, similar to positive Coulomb stress directions, SW-NE for the first main shock and E-W directional horizontal displacements for the second main shock occurred. It was observed that horizontal displacements reached ~6 m, especially along the fault zones where the rupture occurred (green continuous line).

6. Conclusions

Modeling results based on Coulomb stress analysis after the earthquakes defined as 06 February 2023 Kahramanmaraş earthquakes explain the formation of the earthquake sequence occurring in the EAFZ of the elastic stress transfer. Especially the fact that the earthquake occurred at a shallow depth caused higher energy to reach the surface and the stress transfer to take place in a short time. How-

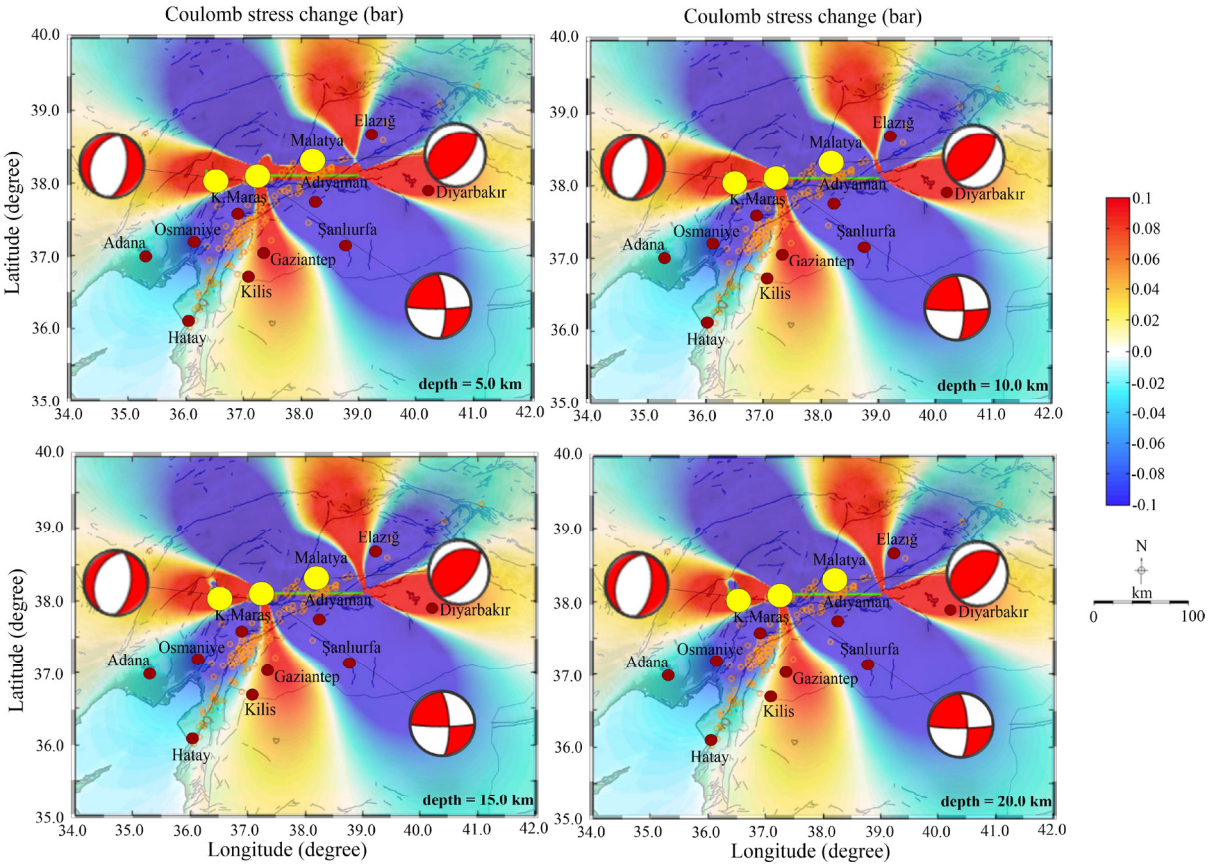

Figure 6. Coulomb stress changes due to the earthquakes (M_w = 7.6, M_L = 5.7, and M_w = 5.9) that occurred around the Kahramanmaraş and Malatya for the depths of 5.0, 10.0, 15.0, and 20.0 km. The big yellow circles show the epicenter of the earthquakes with the focal mechanism results taken from the AFAD website (https://deprem.afad.gov.tr/event-catalog). The orange circles depict epicentral locations of aftershocks that occurred from 06.02.2023 at 01:17:32 (UTC) to 06.02.2023 at 10:51:30 (UTC). Claret red circles show the city centers. Black lines represent the active faults (modified from Emre et al. (2018)).

ever, the only and most important reason for the very high damage caused by earthquakes was not the complex faulting system, but mostly old and unstable construction which was not built in accordance with the soil conditions.

In order to follow the change in stress during the study and to understand whether the stress failure is as expected in a very short time, first of all, Coulomb stress analysis of the earthquakes (M_w = 7.7) and (M_w = 6.6) was made for 5, 10, 15, and 20 km depths and was observed that the stresses increased in the direction of Malatya-Adıyaman in the northeast, Elbistan-Göksun in the northwest, Hatay-Syria border in the south and İskenderun Bay in the southwest. Coulomb analysis was made for 5, 10, 15, and 20 km depths for earthquakes that occurred in Ekinözü-Elbistan (Kahramanmaraş) (M_w = 7.6) in the west, Yeşilyurt (Malatya) (M_L = 5.7) in the direction of Malatya-Adıyaman and Göksun (Kahramanmaraş) (M_w = 5.9) in the west direction of Göksun-Elbistan where the stresses in the previous analysis increased and were observed increased in stress between Elazığ-Diyarbakır in the northeast, between Malatya-Elazığ in the north and Gaziantep-Kilis in the south. Then, on February 20, 2023, an earthquake of M_w = 6.4 in Defne-Hatay occurred and this earthquake was evaluated as the failure of the tension in the direction of the Hatay-Syria border in the south. After that, a combined Coulomb analysis of six earthquakes is made and the current stress distribution at the time of this study is observed as the regions where stresses are transferred between Elazığ and Malatya in the northeast, Kahramanmaraş-Göksun in the west, Hatay and Syria border in the south, and İskenderun Bay in the southwest. The vertical and horizontal displacements of the focal mechanism solution of two main shocks with M_w = 7.7 and M_w = 7.6 magnitudes also provided confirmatory results in terms of showing the variation of stress directions and their depths.

The absence of a major earthquake in this segment of

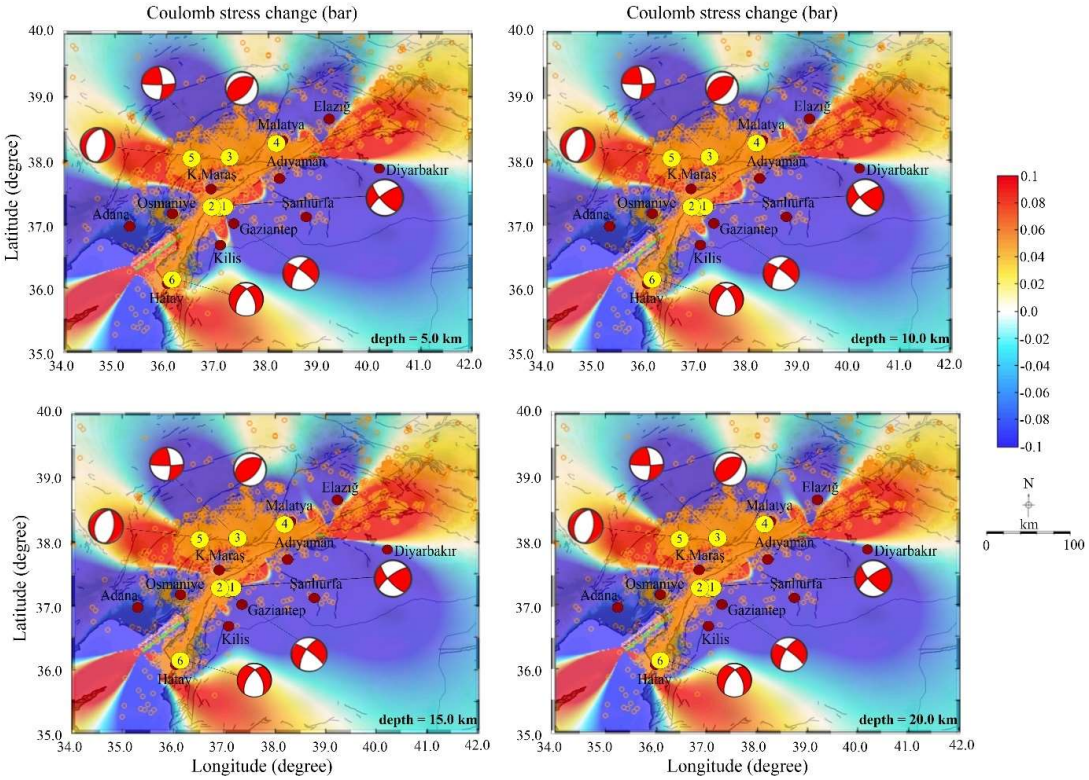

Figure 7. Coulomb stress changes of all induced shocks for the depths of 5.0, 10.0, 15.0, and 20.0 km. The big yellow circles show the epicenter location of the earthquakes with the focal mechanism results taken from the AFAD website (https://deprem.afad.gov.tr/event-catalog). The number above each earthquake is given in Table. The orange circles depict epicentral locations of aftershocks that occurred from February 06, 2023, to February 23, 2023. Claret red circles show the city centers. Black lines represent the active faults (modified from Emre et al. (2018)).

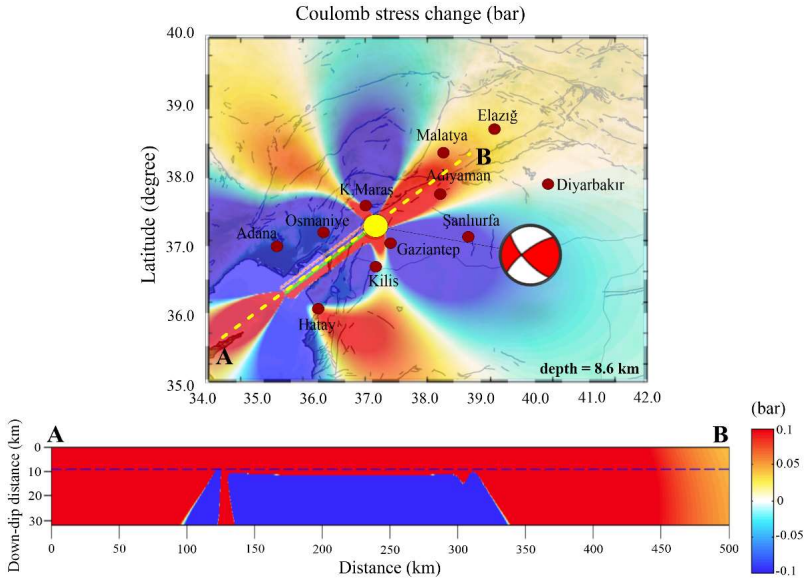

Figure 8. The vertical cross-section of Coulomb stress changed along profile A-B during the Pazarcık earthquake ($M_w = 7.7$) at a depth of 8.6 km. The catalog information is taken from the AFAD website (https://deprem.afad.gov.tr/event-catalog).

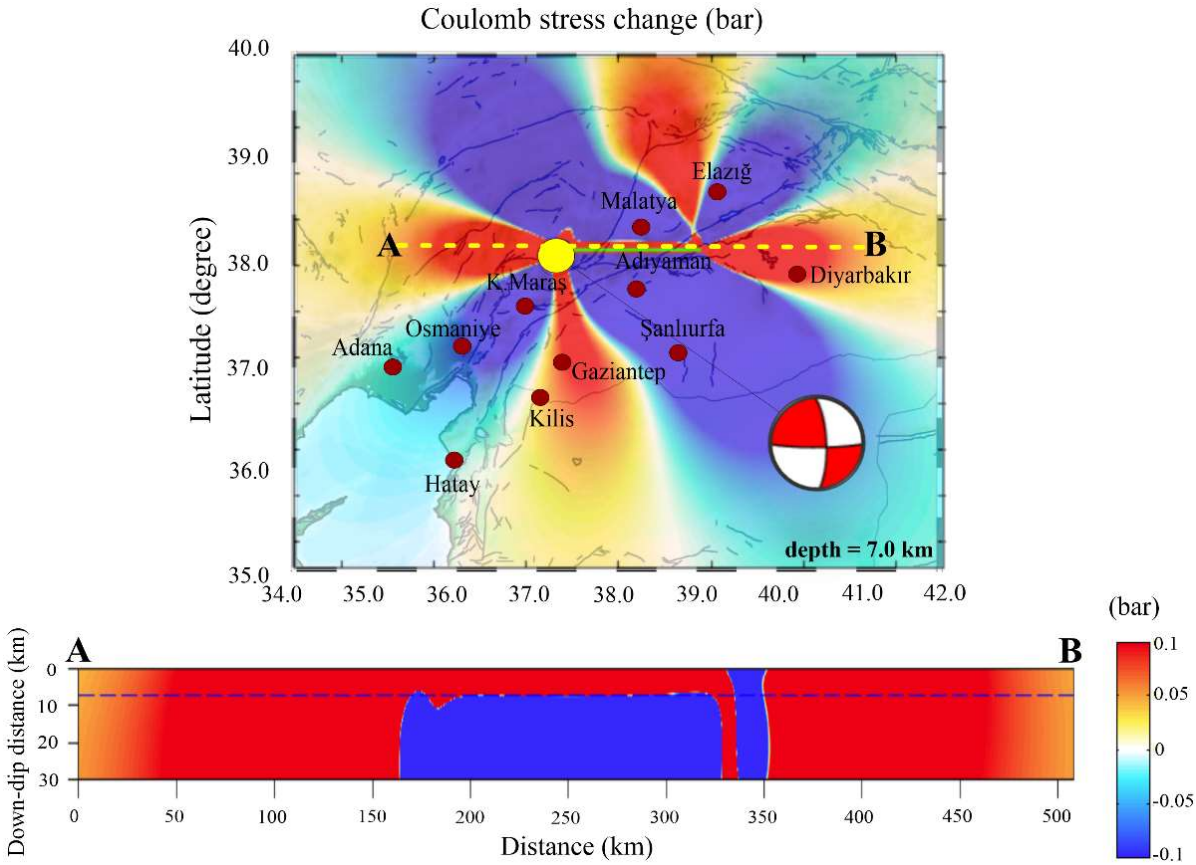

Figure 9. The vertical cross-section of Coulomb stress changed along profile A-B during the Elbistan earthquake (M_w = 7.6) at a depth of 7.0 km. The catalog information is taken from the AFAD website (https://deprem.afad.gov.tr/event-catalog).

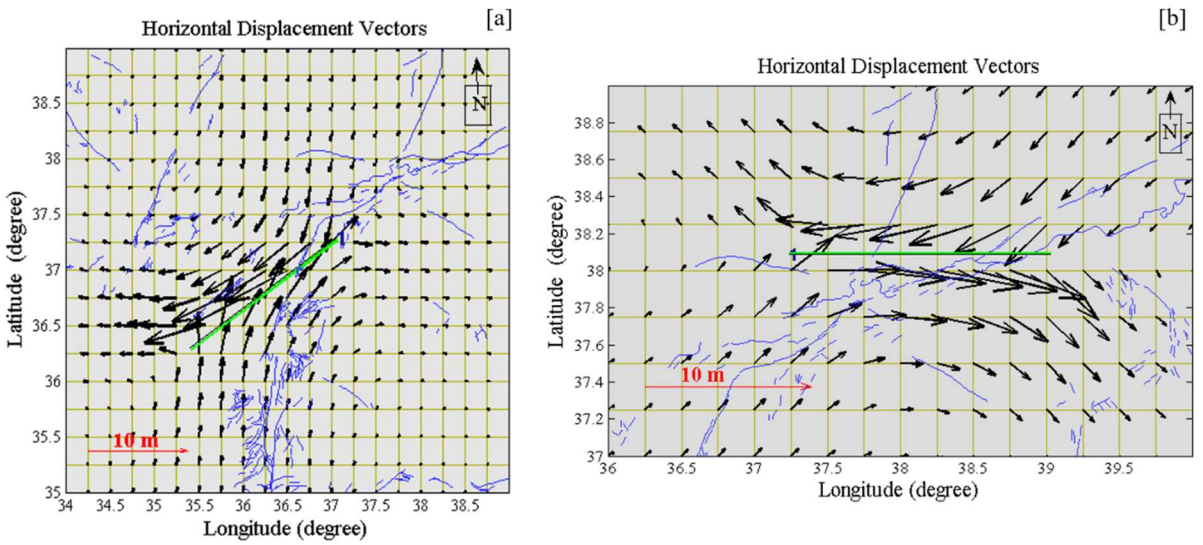

Figure 10. The horizontal displacement vector analyses for (a) the Pazarcık earthquake (M_w = 7.7) and (b) the Elbistan earthquake (M_w = 7.6). Blue lines depict active fault zones taken by Emre et al. (2018).

the EAFZ for a long time has caused great tension in this region and the rupture to occur with very high energy.

Acknowledgments
We thank the anonymous reviewer for his/her interest in this work and for critically reviewing the manuscript. The authors thank the Kandilli Observatory and Earthquake Research Institute (KOERI) and the Disaster and Emergency Management Authority (AFAD) for providing earthquake catalogs. Some of the figures are plotted by using the Generic Mapping Tools (Wessel et al., 2019) software package. The active fault database is taken from Emre et al. (2018).

References

AFAD (2023). The Disaster and Emergency Management Authority (AFAD) Earthquake Catalog. AFAD | deprem.gov.tr. Access date: 20.02.2023

Aktug BA, Ozener H, Dogru A, Sabuncu A, Turgut B et al. (2016). Slip rates and seismic potential on the East Anatolian Fault System using an improved GPS velocity field. Journal of Geodynamics 1(94): 1-2. https://doi.org/10.1016/j.jog.2016.01.001

Alkan H, Büyüksaraç A, Bektaş Ö, Işık E (2021). Coulomb stress change before and after 24.01. 2020 Sivrice (Elazığ) Earthquake (Mw = 6.8) on the East Anatolian Fault Zone. Arabian Journal of Geosciences 14 (23): 1-12. https://doi.org/10.1007/s12517-021-09080-1

Altunel E, Meghraoui M, Karabacak V, Akyüz SH, Ferry M et al. (2009). Archaeological sites (tell and road) offset by the Dead Sea Fault in the Amik Basin, southern Turkey. Geophysical Journal International 179 (3): 1313-1329. https://doi.org/10.1111/j.1365-246X.2009.04388.x

Ambraseys NN (1970). Some characteristic features of the Anatolian fault zone. Tectonophysics 9 (2-3): 143-165.

Ambraseys NN, Barazangi M (1989). The 1759 earthquake in the Bekaa Valley: implications for earthquake hazard assessment in the Eastern Mediterranean region. Journal of Geophysical Research Solid Earth B4: 4007-4013. https://doi.org/10.1029/JB094iB04p04007.

Ambraseys NN, Jackson JA (1998). Faulting associated with historical and recent earthquakes in the Eastern Mediterranean region. Geophysical Journal International 133: 390-406.

Ansari S (2016). Co-seismic stress transfer and magnitude-frequency distribution due to the 2012 Varzaqan-Ahar earthquake doublets (Mw 6.5 and 6.4), NW Iran. Journal of Asian Earth Sciences 132: 129-137. https://doi.org/10.1016/j.jseaes.2016.10.006

Antonioli A, Piccinini D, Chiaraluce L, Cocco M (2005). Fluid flow and seismicity pattern: evidence from the 1997 Umbria-Marche (central Italy) seismic sequence. Geophys Research Letters 32: L10311. https://doi.org/10.1029/2004GL022256

Barka AA (1999). The 17 August 1999 Izmit earthquake. Science 285: 1858-1859.

Bayrak E, Bayrak Y, Yilmaz Ş, Softa M, Turker T (2015). Earthquake hazard analysis for East Anatolian Fault Zone, Turkey. Natural Hazards 76: 1063-1077. https://doi.org/10.1007/s11069-014-1541-5

Bozkurt E (2001). Neotectonics of Turkey-a synthesis. Geodinamica Acta 14 (1-3): 3–30.

Bulut F, Bohnhoff M, Eken T, Janssen C, Kılıç T et al. (2012). The East Anatolian Fault Zone: Seismotectonic setting and spatiotemporal characteristics of seismicity based on precise earthquake locations. Journal of Geophysical Research 117: B07304. https://doi.org/10.1029/2011JB008966

Chinnery MA (1963). The stress changes that accompany strike-slip fault- ing. Bulletin of the Seismological Society of America 53: 921-932.

Çetin H, Güneyli H, Mayer L (2003). Paleoseismology of the Palu-Lake Hazar Segment of the East Anatolian Fault Zone, Turkey. Tectonophysics 374: 163-197. https://doi.org/10.1016/j.tecto.2003.08.003

Çakır Z, Barka AA, Evren E (2003). Coulomb Stress Interactions and the 1999 Marmara Earthquakes. Turkish Journal of Earth Sciences 12: 1. https://journals.tubitak.gov.tr/earth/vol12/iss1/6

Duman TY, Emre Ö (2013). The East Anatolian Fault: geometry, segmentation and jog characteristics. Geological Society London Special Publications 372 (1): 495-529. https://doi.org/10.1144/SP372.14

Emre Ö, Duman TY, Özalp S, Şaroğlu F, Olgun Ş et al. (2018). Active fault database of Turkey. Bulletin of Earthquake Engineering 16 (8): 3229-3275. https://doi.org/10.1007/s10518-016-0041-2

Ergin K, Guglu U, Uz Z (1967). A catalogue of earthquakes of Turkey and surrounding area (11 A.D. to 1964 A.D.). Maden Fakültesi Arz Fiziği Enstitüsü Yayin Istanbul 24: 169.

Gülerce Z, Shah ST, Menekşe A, Özacar AA, Kaymakci N et al. (2017). Probabilistic Seismic-Hazard Assessment for East Anatolian Fault Zone Using Planar Fault Source Models. *Bulletin of the Seismological Society of America* 107 (5): 2353-2366. https://doi.org/10.1785/0120170009

Harris R (1998). Introduction to special section: Stress triggers, stress shadows, and implications for seismic hazard. Journal of geophysical research 103 (10): 24347-24358.

Irmak TS, Toker M, Yavuz E, Şentürk E, Güvenaltın MA (2021). New insight into the 24 January 2020, Mw 6.8 Elazığ earthquake (Turkey): An evidence for rupture-parallel pull-apart basin activation along the East Anatolian Fault Zone constrained by Geodetic and Seismological data. Annals of Geophysics 64 (4): SE439-. https://doi.org/10.4401/ag-8638

Kartal RF, Kadirioğlu FT (2013). Doğu Anadolu Fayının sismotektoniği ve bu fay üzerindeki son beş yıllık deprem aktivitesinin istatistiksel analizi. 66. Türkiye Jeoloji Kurultayı, 01-05 Nisan 2013, ODTÜ Kültür ve Kongre Merkezi, Ankara (in Turkish).

King GC, Stein RS, Lin J (1994). Static stress changes and the triggering of earthquakes. Bulletin of the Seismological Society of America 84 (3): 935-953. https://doi.org/10.1785/BSSA0840030935

King GCP, Cocco M (2001). Fault interaction by elastic stress changes: new clues from earthquake sequences. Advances in Geophysics 44: 1-38. https://doi.org/10.1016/S0065-2687(00)80006-0

Lin J, Stein RS (2004). Stress triggering in thrust and subduction earthquakes, and stress interaction between the southern San Andreas and nearby thrust and strike-slip faults. Journal of Geophysical Research B02303. https://doi.org/10.1029/2003JB002607

Mahmoud Y, Masson F, Meghraoui M, Cakir Z, Alchalbi A et al. (2013). Kinematic study at the junction of the East Anatolian fault and the Dead Sea fault from GPS measurements. Journal of Geodynamics 67: 30-39. https://doi.org/10.1016/j.jog.2012.05.006

McClusky S, Balassanian S, Barka A, Demir C, Ergintav S et al. (2000). Global Positioning System constraints on plate kinematics and dynamics in the eastern mediterranean and Caucasus. Journal of Gephysical Research 105: 5695- 5719.

Nalbant SS, McCloskey J, Steacy S, Barka AA (2002). Stress accumulation and increased seismic risk in eastern Turkey. Earth and Planetary Science Letters 195 (3-4): 291-8. https://doi.org/10.1016/S0012-821X(01)00592-1

Nalbant S, Steacy S, Sieh K, Natawidjaja D, McCloskey J (2005). Earthquake risk on the Sunda trench. Nature 435: 756–757. https://doi.org/10.1038/nature435756a

Okay AI, Tüysüz O (1999). Tethyan sutures of northern Turkey. Geological Society London Special Publications 156 (1): 475-515. https://doi.org/10.1144/GSL.SP.1999.156.01.22

Over S, Ozden S, Yilmaz H (2004). Late Cenozoic stress state distributions along the Karasu Valley, SE Turkey. Tectonophysics 380: 43-68.

Över S, Ünlügenç UC, Bellier O (2002). Quaternary stress regime change in the Hatay region (SE Turkey). Geophysical Journal International 148: 649-662.

Öztürk S (2020). A study on the variations of recent seismicity in and around the Central Anatolian region of Turkey. Physics of the Earth and Planetary Interiors 30: 106453. https://doi.org/10.1016/j.pepi.2020.106453

Poirier JP, Taher MA (1980). Historical seismicity in the near and Middle East, North Africa, and Spain from Arabic documents (VIIth-XVIIIth century). Bulletin of the Seismological Society of America 70 (6): 2185-2201.

Reilinger R, McClusky S, Vernant P, Lawrence S, Ergintav S et al. (2006). GPS constraints on continental deformation in the Africa-Arabia-Eurasia continental collision zone and implications for the dynamics of plate interactions. Journal of Geophysical Research: Solid Earth 111 (B5): B05411. https://doi.org/10.1029/2005JB004051

Reilinger R, McClusky S, Vernant P, Lawrence S, Ergintav S et al. (2006). GPS constraints on continental deformation in the Africa-Arabia-Eurasia continental collision zone and implications for the dynamics of plate interactions. Journal of Geophysical Research: Solid Earth 111 (B5).

Reilinger R, McClusky S (2011). Nubia-Arabia-Eurasia plate motions and the dynamics of Mediterranean and Middle East tectonics. Geophysical Journal International 186 (3): 971-979. https://doi.org/10.1111/j.1365-246X.2011.05133.x

Shapiro SA, Patzig R, Rothert E, Rindshwentner J (2003). Triggering of seismicity by pore pressure perturbations: permeability-related signature of the phenomenon. Pure and Applied Geophysics 160: 1051-1066. https://doi.org/10.1007/978-3-0348-8083-1_16

Sieberg A (1932). Erdbebengeographie. Handbuch der Geophysik 4: 708-744.

Soysal H, Sipahioglu S, Kolcak D, Altinok Y (1981). Türkiye ve çevresinin tarihsel deprem katalogu. TUBITAK Proje no. TBAG 341 Istanbul 86 (in Turkish).Stein RS, King GC, Lin J (1994). Stress triggering of the 1994 M = 6.7 Northridge, California, earthquake by its predecessors. Science 265 (5177): 1432-1435.

Stein RS, Barka AA, Dieterich JH (1997). Progressive failure on the North Anatolian fault since 1939 by earthquake stress triggering. Geophysical Journal International 128 (3): 594604. https://doi.org/10.1111/j.1365-246X.1997.tb05321.x

Şengör AMC, Görür N, Şaroğlu F (1985). Strike-slip faulting and related basin formation in zones of tectonic escape: Turkey as a case study. in: Biddle K.T., ChristieBlick N. (Eds.), Strike-slip Faulting and Basin Formation, Society of Economic Paleontologists and Mineralogists 37: 227-264.

Toda S, Stein RS, Reasenberg PA, Dieterich JH, Yoshida A (1998). Stress transferred by the 1995 Mw = 6.9 Kobe, Japan, shock: Effect on aftershocks and future earthquake probabilities. Journal of Geophysical Research Solid Earth 103 (B10): 24543-24565. https://doi.org/10.1029/98JB00765

Toda S, Stein RS, Lin J (2011). Widespread seismicity excitation throughout central Japan following the 2011 M = 9.0 Tohoku earthquake and its interpretation by Coulomb stress transfer. Geophysical Research Letters 38 (7). https://doi.org/10.1029/2011GL047834

Wessel P, Luis J, Uieda L, Scharroo R, Wobbe F et al. (2019). The Generic Mapping Tools Version 6. Geochemistry Geophysics Geosystems 20.

Westaway R (2004). Kinematic consistency between the Dead Sea Fault Zone and the Neogene and Quaternary left-lateral faulting in SE Turkey. Tectonophysics 391: 203-237. https://doi.org/10.1016/j.tecto.2004.07.014

Willis B (1928). Earthquakes in the Holy Land. Bulletin of the Seismological Society of America 18 (2): 73-103. https://doi.org/10.1785/BSSA0180020073

Yildiz H, Cirmik A, Pamukcu O, Özdağ ÖC, Gönenç T et al. (2021). 12th June 2017 offshore Karaburun-Lesvos Island earthquake coseismic deformation analysis using continuous GPS and seismological data. Turkish Journal of Earth Sciences 30 (3): 341-358. https://doi.org/10.3906/yer-2008-3

Supplementary Material for

Investigation of Earthquake Sequence and Stress Transfer in the Eastern Anatolia Fault Zone by Coulomb Stress Analysis

Hamdi ALKAN[1,*], Aydın BÜYÜKSARAÇ[2], Özcan BEKTAŞ[3]

Contents of this file
Tables S1 to S2:
- S1: Destructive earthquakes around the EAFZ in the historical period
- S2: Earthquakes with a magnitude greater than 5.0 around the EAFZ in the instrumental period

Table S1. Destructive earthquakes around the EAFZ in the historical period (compiled from AFAD and KOERI websites, respectively, https://deprem.afad.gov.tr/event-historical and http://www.koeri.boun.edu.tr/sismo/2/en/)

Date	Latitude (°)	Longitude (°)	Intensity	Location	Service
69	36.25	36.10	IX	Antakya	KOERI
115	36.25	36.10	IX	Antakya	KOERI
245	36.25	36.10	X	Antakya	KOERI
334	36.25	36.10	IX	Antakya	KOERI
506	36.25	36.10	IX	Antakya	KOERI
526	36.25	36.10	IX	Antakya	KOERI
529	36.25	36.10	IX	Antakya	KOERI
587	36.25	36.10	IX	Antakya	KOERI
859	36.25	36.10	IX	Antakya	KOERI
867	36.25	36.10	IX	Antakya	KOERI
1003	36.37	37.51	VIII	Urfa	AFAD
1037	36.37	37.51	VII	Urfa	AFAD
1042	36.50	37.90	VIII	Munbiç	AFAD
1053	36.25	36.10	VIII	Antakya	AFAD
1089	36.50	37.90	VIII	Munbiç	AFAD
1091	36.25	36.10	VII	Antakya and Urfa	AFAD
1109	36.50	37.90	VIII	Munbiç	AFAD
1114	36.50	35.50	IX	İskenderun	KOERI
1137	36.20	37.15	X	Mezopotamya	AFAD
1138	36.30	37.20	VIII	Mezopotamya	AFAD
1156	36.21	37.15	VIII	Halep	AFAD
1190	36.25	36.10	VIII	Antakya	AFAD
1204	36.20	37.10	VIII	Halep, Tire	AFAD
1205	38.70	35.50	VIII	Kayseri	AFAD
1268	37.35	35.80	IX	Ceyhan	KOERI
1287	35.60	35.72	VIII	Lazkiye	AFAD
1404	36.30	37.00	VII	Halep	AFAD
1544	38.00	37.00	VIII	Elbistan	AFAD
1568	35.60	36.00	VII	Lazkiye	AFAD
1717	38.70	35.50	VIII	Kayseri	AFAD
1719	36.20	37.10	IX	Halep	AFAD

Table S1. (Continued)

1738	36.25	36.10	VII	Antakya	AFAD
1752	35.60	35.75	IX	Lazkiye	AFAD
1779	38.35	38.30	VIII	Malatya	AFAD
1783	35.52	35.79	VIII	Tripoli	AFAD
1789	38.70	39.90	VIII	Palu	AFAD
1795	36.20	37.10	VII	Halep	AFAD
1796	35.61	36.00	VIII	Lazkiye	AFAD
1822	36.40	36.20	IX	İskenderun	KOERI
1831	36.20	37.10	VII	Halep	AFAD
1835	38.72	35.50	VIII	Kayseri	AFAD
1837	35.65	36.82	X	Suriye	AFAD
1854	36.20	36.60	VII	Antakya	AFAD
1866	38.50	40.90	IX	Kulp	AFAD
1866	38.40	39.40	VIII	Hazar Lake	AFAD
1872	36.25	36.10	X	Antakya	KOERI
1874	38.50	39.50	IX	Elazığ	AFAD
1875	36.20	36.10	VII	Antakya	AFAD
1875	39.30	41.00	VIII	Karlıova	AFAD
1884	36.30	37.20	VII	Halep	AFAD
1893	37.03	37.24	IX	Malatya	AFAD
1895	38.73	35.47	IX	Kayseri	AFAD

Table S2. Earthquakes with a magnitude greater than 5.0 around the EAFZ in the instrumental period (compiled from the USGS website https://www.usgs.gov/programs/earthquake-hazards/earthquakes)

No	**Date (UTC)**	**Latitude (°N)**	**Longitude (°E)**	**Depth (km)**	**Magnitude (Mw)**
1	1905-12-04 07:05:30	38.153	38.645	10	6.8
2	1905-12-04 12:20:07	37.216	38.830	15	5.6
3	1907-06-03 06:45:11	38.094	41.878	15	5.3
4	1914-05-28 11:27:28	39.696	35.988	15	5.8
5	1915-05-19 04:48:30	38.400	39.674	15	5.7
6	1915-12-25 06:06:09	36.428	36.166	15	5.5
7	1918-09-29 12:07:15	35.075	35.462	15	6.4
8	1919-05-27 10:34:27	37.378	35.801	15	5.7
9	1923-04-29 09:34:41	39.934	36.367	15	5.9
10	1924-09-13 14:34:16	39.938	41.876	15	6.9

Table S2. (Continued)

11	1929-09-27 04:27:46	39.880	41.472	15	5.6
12	1928-08-23 06:16:06	37.402	35.620	15	5.3
13	1929-05-16 01:22:32	35.494	35.377	15	5.2
14	1929-09-15 13:10:06	39.697	39.029	15	5.5
15	1930-02-08 05:20:06	37.757	39.012	15	5.3
16	1930-12-10 10:31:30	39.972	39.152	15	5.8
17	1931-05-06 20:22:21	38.436	38.955	15	5.2
18	1934-11-12 07:19:14	38.302	40.934	15	6.0
19	1935-10-13 19:32:18	39.110	40.582	15	5.5
20	1936-06-14 17:01:32	36.543	35.867	15	5.7
21	1937-12-07 09:30:57	39.475	39.918	15	5.2
22	1939-12-26 23:57:23	39.907	39.586	20	7.8
23	1940-02-03 19:34:56	39.804	37.799	15	5.1
24	1940-04-13 06:29:10	39.531	35.446	15	5.8
25	1940-04-22 12:20:43	39.311	39.963	15	5.5
26	1940-05-29 15:24:45	39.040	40.562	15	5.5
27	1940-07-30 00:12:11	39.833	35.476	15	6.2
28	1940-07-31 10:36:33	39.696	35.639	15	5.4
29	1940-09-23 19:30:22	39.020	39.505	15	5.2
30	1941-04-27 13:01:27	39.646	35.728	15	6.0
31	1941-11-12 10:04:54	39.782	39.506	15	6.0
32	1943-11-29 18:45:38	38.540	41.475	15	5.8
33	1945-03-20 07:58:52	37.244	35.859	15	6.1
34	1946-05-31 03:12:46	39.230	41.374	15	5.9
35	1947-12-09 23:40:01	36.511	34.751	15	5.8
36	1948-08-18 19:06:13	38.390	39.141	15	5.4
37	1949-04-25 23:09:12	37.915	39.234	15	5.5

Table S2. (Continued)

38	1949-08-17 18:44:17	39.503	40.671	15	6.8
39	1949-08-17 20:45:26	39.218	40.717	15	5.5
40	1949-08-23 13:40:44	39.174	41.128	15	5.3
41	1950-05-09 09:20:03	38.039	38.515	15	5.4
42	1951-04-08 21:38:10	36.516	35.869	15	5.8
43	1952-10-22 17:00:41	36.841	35.496	15	5.7
44	1953-03-24 21:17:36	36.855	36.966	15	5.5
45	1957-07-07 05:58:52	39.067	40.410	15	5.5
46	1959-09-10 13:59:15	39.287	41.463	15	5.4
47	1959-10-25 15:57:55	39.177	41.599	15	5.4
48	1963-08-25 06:11:46	39.019	38.477	35	5.3
49	1964-04-23 14:23:45	38.203	38.964	15	5.2
50	1964-06-14 12:15:34	38.205	38.622	10	5.8
51	1964-06-14 12:38:02	38.006	38.580	15	5.2
52	1964-09-04 03:39:35	39.662	40.364	15	5.2
53	1964-11-16 05:27:28	39.454	40.489	15	5.2
54	1965-05-16 11:29:41	38.233	39.061	15	5.2
55	1965-08-31 07:29:49	39.430	40.763	15	5.4
56	1966-03-07 01:16:09	39.174	41.627	15	5.4
57	1966-08-19 12:22:12	39.235	41.572	24.7	6.8
58	1966-08-19 13:54:23	39.024	41.813	10	5.4
59	1966-08-19 14:17:54	39.309	41.302	10	5.3
60	1966-08-19 18:41:14	39.127	41.493	10	5.1
61	1966-08-20 11:59:13	39.438	41.094	25	6.2
62	1966-08-20 12:01:41	39.140	40.868	10	5.6
63	1967-13-30 12:24:58	39.280	41.324	10	5.1
64	1967-04-07 17:07:13	37.374	36.158	15	5.2

Table S2. (Continued)

65	1967-04-07 18:33:30	37.313	36.243	15	5.3
66	1967-07-26 18:53:02	39.568	40.445	20	6.2
67	1967-10-20 06:47:34	38.022	38.714	15	5.1
68	1968-09-24 04:19:55	39.142	40.361	10	5.3
69	1968-09-25 20:52:13	39.231	40.406	10	5.4
70	1968-10-30 16:51:38	37.991	38.529	15	5.3
71	1969-09-10 12:13:58	39.217	41.465	15	5.5
72	1969-10-01 20:33:38	39.336	40.626	15	5.2
73	1970-09-03 05:32:10	39.624	38.822	15	5.3
74	1971-05-22 16:44:02	38.934	40.653	10	6.6
75	1971-05-22 17:34:18	39.040	40.278	15	5.1
76	1971-05-22 18:35:28	38.997	40.729	10	5.1
77	1971-06-29 09:08:14	37.111	36.905	35	5.3
78	1971-07-11 20:12:56	37.181	36.778	10	5.8
79	1971-08-17 04:29:36	37.089	36.851	42.5	5.3
80	1975-09-06 09:20:10	38.474	40.723	26	6.7
81	1975-09-06 10:13:08	38.539	40.589	33	5.1
82	1975-09-06 10:52:15	38.428	40.830	33	5.2
83	1976-09-05 22:07:34	38.298	40.853	22	5.1
84	1977-03-25 02:39:58	38.562	40.024	21	5.2
85	1978-12-04 03:12:34	38.070	37.468	10	5.1
86	1979-09-12 16:14:51	38.662	39.803	10	5.0
81	1979-12-28 03:09:07	37.470	35.847	41	5.1
82	1980-07-11 12:33:25	38.425	40.897	10	5.0
83	1980-10-18 03:14:10	39.851	40.254	35	5.0
84	1981-01-20 08:27:46	38.079	38.473	10	5.1
85	1982-03-27 19:57:23	39.167	41.899	33	5.4

Table S2. (Continued)

86	198-04-06 07:35:46	39.882	40.411	10	5.0
87	1983-11-18 01:15:35	39.781	39.463	27.1	5.0
88	1986-05-05 03:335:38	37.993	37.806	9.6	6.1
89	1986-06-06 10:39:46	38.001	37.917	10	5.8
99	1986-08-03 01:33:20	37.200	37.300	11.5	5.0
100	1989-05-20 20:44:02	39.553	40.172	38.2	5.4
101	1989-06-24 03:09:57	36.719	35.943	41.6	5.1
102	1991-04-10 01:08:39	37.359	36.221	10	5.4
103	1992-03-13 17:18:39	39.710	39.605	27.2	6.7
104	1992-03-15 16:16:24	39.532	39.929	20.9	5.9
105	1992-05-07 19:15:03	38.698	40.143	18.3	5.2
106	1993-06-14 1959:42	39.624	38.410	26.1	5.0
107	1994-01-03 21:00:31	37.002	35.842	25.8	5.0
108	1994-09-17 02:24:37	37.885	41.584	8.8	5.1
109	1994-11-20 14:31:02	35.335	39.557	28.8	5.4
110	1995-01-29 04:16:56	39.830	40.657	31.1	5.2
111	1995-12-05 18:49:30	39.440	40.153	14.9	5.8
112	1995-12-05 18:52:37	39.553	40.190	10	5.3
113	1997-01-22 17:57:18	36.250	35.951	10	5.7
114	1997-01-22 18:24:50	36.239	35.922	10	5.1
115	1997-01-22 18:27:29	36.275	35.997	10	5.3
116	1998-04-13 15:14:33	39.238	41.055	33	5.3
117	1998-05-09 15:38:00	38.278	38.988	10	5.1
118	1998-06-27 13:55:52	36.878	35.307	33	6.3
119	1998-07-04 02:15:46	36.874	35.321	33	5.4
120	199-04-06 00:08:22	39.400	38.307	10	5.4
121	2001-06-25 13:28:46	37.238	36.206	5	5.5

Table S2. (Continued)

122	2001-07-01 21:42:08	39.832	41.623	33	5.4
123	2001-10-31 12:33:52	37.249	36.136	10	5.1
124	2003-01-27 05:26:23	39.500	39.878	10	6.1
125	2003-05-01 00:27:04	39.007	40.464	10	6.4
126	2003-07-13 01:48:21	38.288	38.963	10	5.6
127	2004-03-25 19:30:49	39.930	40.812	10	5.6
128	2004-03-28 03:51:10	39.847	40.874	5	5.6
129	2004-08-11 15:48:26	38.377	39.261	7.4	5.7
130	2005-03-12 07:36:12	39.440	40.978	11.1	5.6
131	2005-03-14 01:55:55	39.354	40.890	5	5.8
132	2005-03-23 21:44:53	39.431	40.925	10	5.7
133	2005-06-06 07:41:28	39.220	41.080	10	5.6
134	2005-11-26 15:56:55	38.260	38.814	8.5	5.1
135	2005-12-10 00:09:50	39.394	40.946	10	5.4
136	2006-03-29 22:05:15	35.252	35.427	27.3	5.0
137	2006-07-02 19:39:39	39.274	40.960	3	5.0
138	2007-02-09 02:22:55	38.390	39.043	2.6	5.5
139	2007-02-21 11:05:28	38.318	39.275	6	5.7
130	2007-08-25 22:05:49	39.282	41.124	10	5.3
131	2008-09-03 02:22:47	37.507	38.503	5.7	5.0
132	2008-11-15 14:03:18	38.841	35.524	10	5.1
133	2009-06-17 04:29:12	36.047	36.020	10.4	5.0
134	2009-07-30 07:37:51	39.588	39.726	10	5.0
135	2010-03-08 02:32:34	38.864	39.986	12	6.1
136	2010-03-08 07:47:41	38.709	40.051	10	5.6
137	2010-03-08 10:14:23	38.828	40.119	5	5.2
138	2010-03-08 11:12:10	38.776	40.143	5	5.1

Table S2. (Continued)

139	2010-03-24 14:11:31	38.821	40.138	4.5	5.1
140	2011-06-23 07:34:42	38.578	39.640	6.1	5.2
141	2011-09-22 03:22:36	39.785	38.842	5	5.5
142	2012-07-22 09:26:02	37.546	36.384	7.6	5.0
143	2013-09-17 20:40:51	39.023	41.492	5.3	5.0
144	2015-12-02 23:27:09	39.283	40.255	10	5.4
145	2016-01-10 17:40:49	39.565	34.337	10	5.0
146	2017-03-02 11:07:26	37.616	38.431	10	5.6
147	2018-04-24 00:34:31	37.596	38.514	10	5.2
148	2018-08-19 15:22:14	37.290	36.364	10	5.1
149	2019-04-04 17:31:10	38.300	39.163	10	5.2
150	2020-01-24 17:55:14	38.431	39.061	10	6.7
151	2020-01-25 16:30:11	38.362	39.110	10	5.1
152	2020-02-25 23:03:37	38.349	38.797	10	5.0
153	2020-03-19 17:53:33	38.392	39.073	10	5.2
154	2020-06-05 18:06:21	38.238	38.759	10	5.1
155	2020-06-14 14:24:29	39.423	40.707	10	5.9
156	2020-06-15 06:51:31	39.423	40.748	10	5.5
157	2020-08-04 09:37:37	38.188	38.698	10	5.6
158	2020-09-20 19:08:07	38.018	34.042	10	5.1
159	2020-12-03 05:45:19	37.946	41.697	10	5.0
160	2020-12-27 06:37:32	38.456	39.230	9	5.5
161	2021-06-25 18:28:37	39.187	40.167	3.1	5.4
162	2021-11-19 1240:53	39.827	41.922	6.2	5.1
163	2022-04-09 14:02:15	38.116	38.662	10	5.3
164	2022-10-11 15:48:46	37.261	36.234	10	5.0